Environ. Sci. Technol. **1999**, *33,* 4465−4470

Sorption of Strontium by Bacteria, Fe(III) Oxide, and Bacteria−Fe(III) Oxide Composites

TROY D. SMALL,[†] LESLEY A. WARREN,[†] ERIC E. RODEN,[‡] AND F. GRANT FERRIS*,[†]

Department of Geology, University of Toronto, Toronto, Ontario, Canada M5S 3B1, and Department of Biological Sciences, The University of Alabama, Tuscaloosa, Alabama 35487-0206

This study provides the first quantitative comparison of the sorptive capacities of a bacteria−Fe oxide composite to its individual components. These results have enormous significance for understanding the fate and transport of inorganic contaminants in natural aqueous environments where heterogeneous bacteria−oxide composite solids are commonly found. We quantify Sr^{2+} sorption to the bacteria *Shewanella alga*, *Shewanella putrefaciens*, amorphous hydrous ferric oxide (HFO), and *S. alga* coated with HFO over a range of total Sr^{2+} concentrations (0.005−10 mM) and pH (2.5−11 at 0.5 pH increments), under well controlled laboratory conditions. Significant Sr^{2+} sorption occurred at significantly lower pH values to the bacteria and *S. alga*−HFO composite (5.5−5.9) compared to HFO (7.6). Geochemical modeling using a generalized Langmuir equation showed that the bacteria sorb significantly greater quantities of Sr^{2+} (maximum sorptive capacity: BSr_{max} = 0.079 and 0.075 mmol·g^{-1} for *S. alga* and *S. putrefaciens*, respectively) than the HFO (0.001 mmol·g^{-1}). The observed BSr_{max} for the *S. alga*−HFO composite (0.034 mmol·g^{-1}) was less than the combined sorptive properties of its components (BSr_{max} = 0.041 mmol·g^{-1}), likely reflecting HFO masking of bacterial surface binding sites.

Introduction

Geochemical characterization of reactions at solid surfaces involving dissolved inorganic contaminants, such as metals and radionuclides, has emerged as a central topic of environmental geochemistry. Modeling such reactions using surface complexation theory (SCT) is becoming increasingly widespread in the literature (*1*−*5*) especially for Fe oxide surfaces and amorphous hydrous ferric oxides (HFO) in particular (*1*, *6*−*8*). However, other reactive mineral surfaces such as carbonates (*9*) and manganese oxides (*10*, *11*) have been considered. More recently, the applicability of this approach for describing reactions at bacterial surfaces has been clearly demonstrated (*12*−*14*). These results suggest an underlying robustness of the SCT in modeling interfacial reactions in aqueous environments.

Radionuclides and heavy metals derived from industrial and military sites have been found as common groundwater contaminants (*8*, *15*), and their mobility in subsurface environments is dependent on interactions with inorganic as well as organic solids (*16*). The necessity of considering bacteria in evaluations of contaminant behavior stems from a large body of experimental evidence suggesting the ability of bacteria and other microorganisms to sorb significant quantities of a variety of metals (*12*−*14*, *17*−*19*), in particular Sr^{2+} (*20*−*23*). Their ubiquitous presence in natural environments underscores further their important role in controlling dissolved metal behavior (*24*, *25*). Bacteria metal scavenging properties are important considerations in the determination of contaminant fate, specifically Sr^{2+} that does not sorb strongly to inorganic surfaces such as iron oxides (*6*). Bacterial metal scavenging extends from the presence of acidic functional groups (*26*, *27*), a characteristic that make mineral surfaces such as Fe oxides geochemically reactive. However, in contrast to Fe oxide surfaces that possess only one type of functional surface site (hydroxyl, OH^-) (*7*), bacterial surfaces possess a variety of reactive sites such as carboxylic, phosphoryl, and amino as well as hydroxyl groups (*13*, *28*). The exact type and number of reactive sites associated with structural polymers in cell walls and other cellular materials are species dependent. Thus there is a higher degree of complexity involved in modeling bacterial surfaces, yet emerging evidence suggests that the principles of geochemical equilibria can be applied.

The recent work by Fein et al. (*13*) and Warren and Ferris (*14*) indicate that the equilibrium SCT approach can be used to quantify reactions at bacterial surfaces. What has yet to be investigated in a quantitative, comparative manner is the relative sorptive properties of bacterial and HFO surfaces. Moreover, in natural environments bacterial surfaces are commonly observed to be coated by iron oxides forming a composite solid comprised of intact cells and natural minerals (*29*−*33*). It is therefore important to consider the bacteria−mineral composite as a geochemically reactive solid and to quantify its trace metal scavenging ability as mixed adsorbent systems have been shown to be nonadditive (*34*). The objectives of this work therefore were to quantify the sorption of Sr^{2+}, a common groundwater contaminant, to the bacteria *Shewanella alga* (strain BrY), *Shewanella putrefaciens* (strain CN-32), HFO, and *S. alga* coated with HFO over a range of total Sr^{2+} concentrations and pH, under well controlled laboratory conditions.

Methods

Growth Conditions for *Shewanella* sp. Pure cultures of the bacteria *Shewanella alga* strain BrY and *Shewanella putrefaciens* strain CN-32 (isolated from the deep subsurface by Dr. David Boone, Portland State University) were grown overnight at 37 °C in Trypticase soy broth (TSB, media pH ∼ 7). The two species of *Shewanella* are gram-negative, Fe(III) and Mn(IV) reducing, facultative anaerobes (*19*, *35*−*37*). Prior to use in experiments, the bacterial cultures were washed by centrifugation three times with sterile ultrapure water (UPW) and resuspended in sterile UPW at a pH of ∼7. Bacteria cell concentrations used in the experiments were equivalent to an optical density of 0.4 at 600 nm (approximately 8×10^8 cells/mL = 0.18 g/L; DAPI [4′,6-diamidino-2-phenylindole dihydrochloride] epifluorescence counts on cell suspensions in pure water). The optical densities of the cell suspensions were measured spectrophotometrically at 600 nm using a Milton Roy Spectronic 1001 Plus. Cell viability was evaluated by epifluorescence microscopy direct counting using the LIVE/DEAD Baclight

* Corresponding author phone: (416)978-0526; fax: (416)978-3938; e-mail: ferris@quartz.geology.utoronto.ca.
[†] University of Toronto.
[‡] The University of Alabama.

10.1021/es9905694 CCC: $18.00
Published on Web 11/09/1999

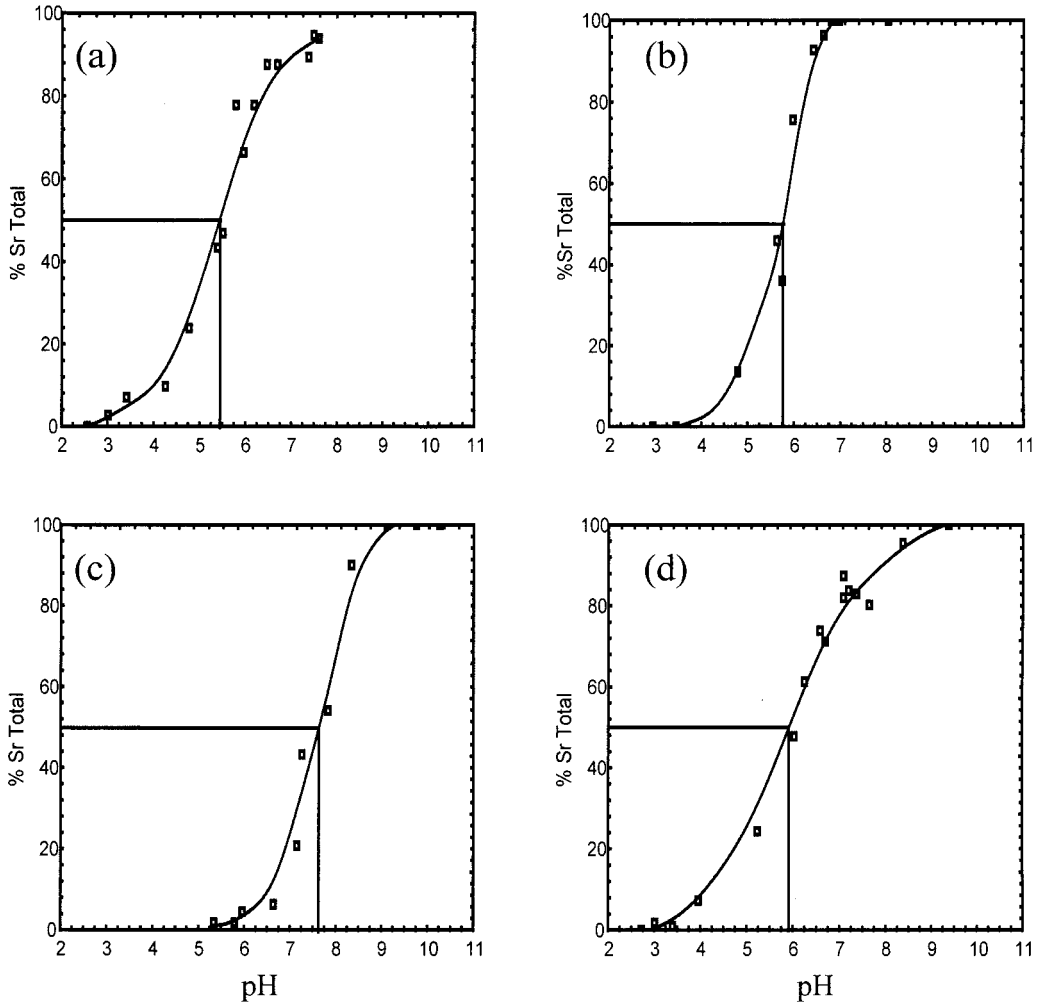

FIGURE 1. Percentage of total strontium ($Sr_T = 10^{-5.5}$ M) sorbed to substrates as a function of pH for (a) *S. alga* (0.18 g/L), (b) *S. putrefaciens* (0.18 g/L), (c) HFO (4.18 g/L), and (*d*) *S. alga*−HFO composite (0.27 g/L) solids. The solid vertical lines indicate the pH at which 50% of the total strontium concentration is being sorbed (pH sorption edges range from 5.5 (*S. alga*) to 7.6 (HFO)).

Bacteria Viability Kit (Molecular Probe Inc. L-7007). Viability counts indicated that the majority (>90%) of the bacterial cells remained intact and viable throughout the sorption experiments.

HFO Preparation. HFO was prepared synthetically in the laboratory by the gradual titration of $Fe(NO_3)_3 \cdot 9H_2O$ with 1 M NaOH to pH 7. The resulting HFO gel precipitate was centrifuged at 7000 rpm for 10 min, rinsed three times, and resuspended in sterile UPW. Total Fe(III) content of the gel was measured by a phenanthroline spectrophotometric assay (HACH DR 2000 spectrophotometer). Fresh HFO was prepared immediately prior to each set of sorption experiments, conducted at an Fe concentration of 45 mM Fe(III), so that any potential changes in the sorptive characteristics of the HFO associated with aging and crystallization were avoided (*6*).

Bacteria−HFO Composites. To prepare *S. alga* cells coated with HFO, *S. alga* cell suspensions were washed and resuspended in UPW as explained above at a cell density equivalent to an $OD_{600\ nm}$ of 0.4 (approximately 8×10^8 cells/mL = 0.18 g/L). An $Fe(NO_3)_3 \cdot 9H_2O$ solution was then added to make a final total Fe concentration of 0.8 mM Fe(III). The solution of *S. alga* cells and 0.8 mM Fe(III) was then gently stirred for 1 h at a pH of ~3 to promote Fe(III) sorption to the bacterial surface. This pH was chosen as it is below the critical pH with respect to supersaturation and precipitation of $Fe(OH)_{3(s)}$ for these experimental conditions (*14*). To achieve HFO precipitation directly at the cell surface it is critical to allow the Fe(III) to sorb first at the bacterial surface before promoting $Fe(OH)_3$ precipitation.

After 1 h the cell-Fe(III) solution was slowly titrated with 1 M NaOH at 0.5 pH unit intervals, with an equilibration time of 15 min at each interval, until a final pH of 7 was reached. The solution was then maintained at this pH and gently shaken for 12 h to allow complete HFO precipitation. Fe(III) was not detected in solution after this period; i.e., all of the Fe(III) added to solution was precipitated as HFO. Scanning electron microscopy (SEM) and energy-dispersive X-ray spectroscopy (EDS) confirmed the presence of iron precipitates at the bacterial surface. X-ray diffraction analyses were used to determine that the HFO precipitates used in these experiments were amorphous in the presence and absence of bacteria.

Strontium Sorption Experiments. Strontium sorption experiments were carried out using the four substrate systems (*S. alga*, *S. putrefaciens*, HFO, and *S. alga*−HFO composite) over a range of Sr^{2+} concentrations (10^{-2}−$10^{-5.5}$ M at $10^{-0.5}$ M increments) and pH (2.5−11 at 0.5 pH increments) under dilute aqueous, nongrowth conditions. Experimental samples were gently shaken at room temperature for 2 h. This relatively short equilibration time (determined through time course experiments) has been shown to maintain cell viability and to approach equilibrium conditions without measurable dissolution of HFO at lower pH values (*14*). After 2 h, the solution pH was measured and used in the calculation of complexation constants, maximum binding capacities, and

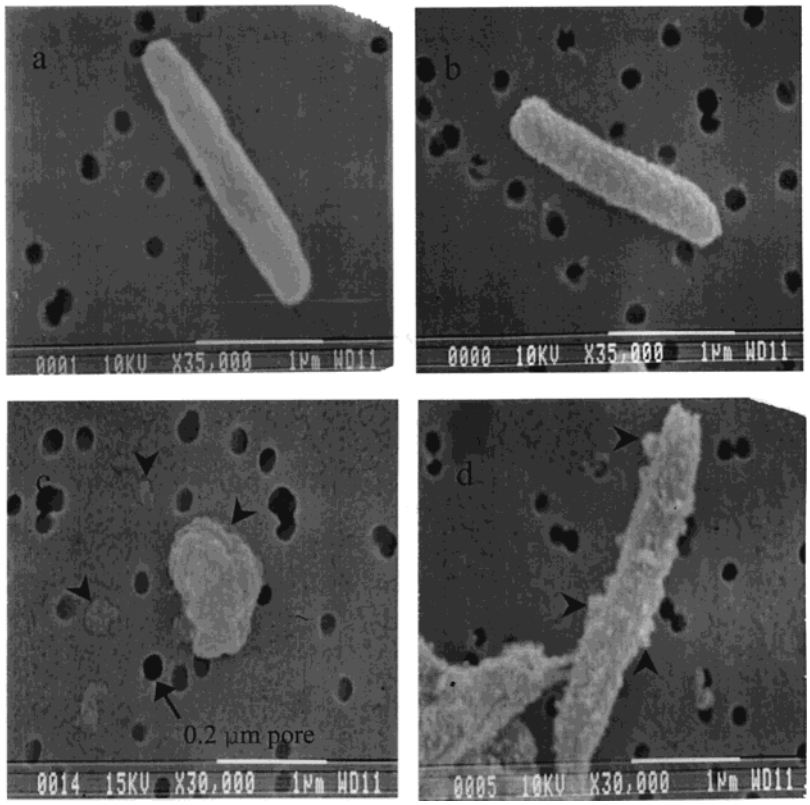

FIGURE 2. Scanning electron micrograph images of substrates exposed to 10^{-3} M Sr^{2+} at pH 9 for (a) *S. alga*, (b) *S. putrefaciens*, (c) HFO, and (d) *S. alga*−HFO composite. Similar cell shapes and sizes were observed for the two species of *Shewanella* (a, b). HFO precipitates (c) are clearly visible (noted by arrows) ranging in diameter from 0.2 to 1.0 μm; when bacteria cells are present (d), the cells are heterogeneously coated with HFO precipitates (noted by arrows).

the construction of pH sorption edge diagrams. The sorption experiments were conducted under dilute aqueous conditions with each of the substrate systems as well as a control (no bacteria or HFO present). Measured concentrations were thus assumed to be equal to activities (*38*) and were subsequently used to calculate Sr^{2+} partitioning. Solid-phase strontium concentrations (Sr_S) were determined by taking the difference between the total Sr^{2+} (Sr_T) and dissolved Sr^{2+} (Sr_D) concentrations. Samples for Sr_D were filtered through 0.22 μm sterile acrodisc filters with a Supor membrane. The experimental solutions were found to be undersaturated with respect to Sr-carbonates and hydroxides over the pH range of the sorption assays (MINEQL+ v. 4).

For each experiment, triplicate 2.5 mL samples were collected for Sr_T and Sr_D analyses. Samples were dispensed into 10 mL acid washed polypropylene tubes to which 0.5 mL of 30% H_2O_2 (Fisher Scientific certified A.C.S.) and 0.1 mL of 70% trace metal grade HNO_3 (Fisher Scientific) were added and heated at 60° C overnight. Following digestion, strontium concentrations were determined using atomic absorption spectrophotometry (AAS) or inductively coupled plasma atomic emission spectroscopy (ICP-AES).

Samples were also collected for visual examination by SEM and elemental analysis using EDS. For this, 1.0 mL subsamples were collected in 1.5 mL eppendorf tubes, centrifuged at 13 000 rpm for 2 min, washed and centrifuged twice more, and then resuspended in 1.0 mL of UPW. The washed bacterial samples were fixed with 2% gluteraldehyde in 0.07 M Sorensen's sodium−potassium phosphate buffer, pH 6.8 (HFO subsamples were not fixed with gluteraldehyde), and vacuum filtered onto a 0.2 μm polycarbonate filter (Nuclepore Track-Etch Membrane). The bacterial samples were subsequently dehydrated through a graded ethanol series (10, 25, 50, 80, 95, 100% ethanol) and subjected to critical point drying in a Toursimis AutoSamdri-814. The samples were then placed on a carbon coated aluminum stub and gold coated with a Cressington Sputter-Coater 108 at 0.06−0.08 mbar for 45 s prior to SEM analyses. The HFO samples were vacuum filtered in the same manner as the bacteria and then air-dried for approximately 4 h. The filters were placed on aluminum stubs and gold coated as described above. Specimens were imaged at 20 kV with a probe current of 10^{-8} to 10^{-9} A in a JEOL 840 scanning electron microscope equipped with a PGT energy-dispersive X-ray spectrophotometer (EDS).

Results and Discussion

Strontium pH Sorption Edges. Sorption of Sr^{2+} to the bacteria, HFO, and bacteria−HFO composite was strongly dependent on solution pH and was initiated by the bacteria and *S. alga*−HFO composite at a much lower pH than the HFO alone (Figure 1). The pH adsorption edge (50% sorption of Sr_T) for *S. alga* occurred at pH 5.5, for *S. putrefaciens* at pH 5.8, for the *S. alga*−HFO composite at pH 5.9, and for HFO at pH 7.6. The *S. alga*−HFO complex exhibited a Sr^{2+} sorption pattern similar to the bacteria alone, i.e., significant sorption of Sr^{2+} occurred at lower pH values than with HFO alone, suggesting that the composite surface still retained bacterial surface functional group reactivity despite the presence of HFO. Significant Sr^{2+} sorption at lower pH values in the presence of bacteria reflects the lower pK_a values associated with functional groups (in particular carboxylic, $pK_a = 4-6$) on the bacterial surface (*13*). Control experiments without sorbent solids revealed no difference between $[Sr_T]$ and $[Sr_D]$ throughout the pH range investigated.

Scanning electron micrograph images noted similar cell shapes and sizes between the two species of *Shewanella* (Figure 2a,b). The HFO precipitates ranged in diameter from 0.2 to 1 μm (Figure 2c). In the *S. alga*−HFO composites,

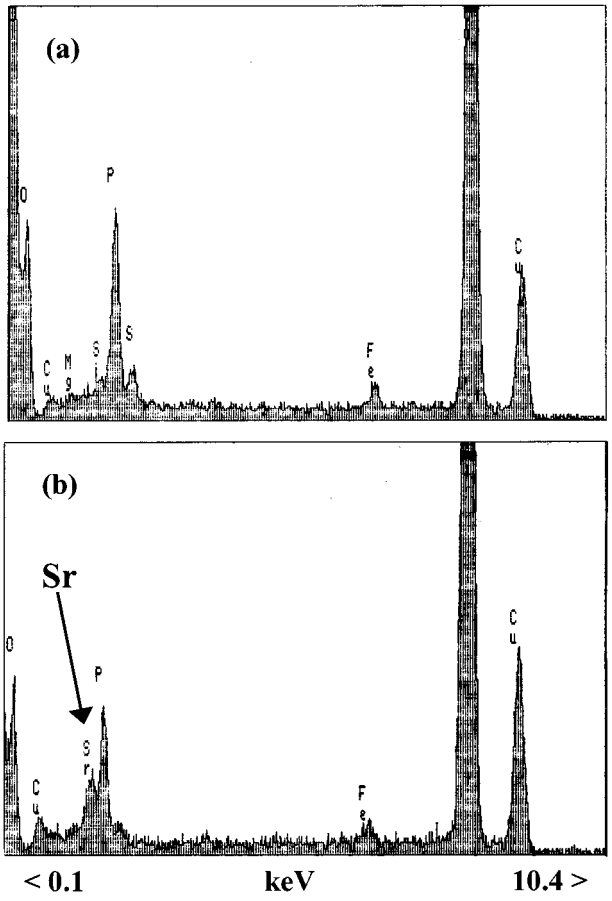

FIGURE 3. Energy-dispersive X-ray spectrum of a *S. alga* cell shown in Figure 2a in UPW (no Sr^{2+} added to solution) (a) and exposed to 10^{-3} M Sr^{2+} at pH 9 (b). The P is from the 2% gluteraldehyde Sorensen buffer used for specimen fixation, and the Fe is retained by the cells from the culture medium. The Cu (Kα and Kβ) peaks are from the specimen support grid.

fine-grained, Fe(III) precipitates were observed on the cells (Figure 2d) suggesting that the bacterial surface served as a nucleation template for HFO precipitation as explained by Warren and Ferris (*14*). Significant bulk HFO precipitation away from the cell surface was not observed. Direct energy-dispersive X-ray spectra analysis of *S. alga* cells identified a distinct Sr^{2+} peak indicative of Sr^{2+} sorption to the bacterial surface (Figure 3).

Strontium Sorption Isotherms. The sorption of Sr^{2+} to either bacterial or iron oxide surfaces can be described using a basic sorption reaction based on the assumption that protonated functional groups (i.e., carboxyl, phosphoryl, hydroxyl) are present on the surface of the sorbing substrate (*1*). An overall mass action expression can be written for Sr^{2+} sorption using a generalized functional group to represent these sorption sites

$$BH + Sr^{2+} \leftrightarrow BSr^{+} + H^{+} \quad (1)$$

where BH represents any protonated functional group, Sr^{2+} represents the solute strontium concentrations, BSr^{+} represents sorbed Sr^{2+}, and H^{+} is the equilibrium proton concentration. The corresponding concentration apparent surface complex formation constant (*6*), K^{S}_{Sr}, is then given by

$$K^{S}_{Sr} = [BSr^{+}][H^{+}]/[BH][Sr^{2+}] \quad (2)$$

where BSr^{+} can be estimated by experimental values of Sr_S, and Sr^{2+} can be estimated by experimental Sr_D concentrations. The corresponding Langmuir equation, in which the mass action reaction for Sr^{2+} sorption is combined with the mass balance equation for the corresponding total number of reactive surface sites, takes the form (*14*)

$$[BSr^{+}] = [BSr_{max}]K^{S}_{Sr}([Sr_D]/[H^{+}])/1 + K^{S}_{Sr}([Sr_D]/[H^{+}]) \quad (3)$$

where BSr^{+} is the concentration of strontium sorbed to the substrate surface, and BSr_{max} is the maximum binding capacity of each reactive surface for Sr^{2+}.

The double logarithmic plots of the experimental equilibrium data show that a relationship exists between solid-phase Sr^{2+} partitioning and $[Sr_D]/[H^{+}]$ for each of the experimental systems (Figure 4). The asymtopic nature of the isotherms suggests that the affinity of Sr^{2+} for sorption changes as surface site saturation is approached. This behavior is consistent with alterations in surface charge that can be anticipated from the sorption of Sr^{2+} according to eq 1, which is dictated by combined chemical and electrostatic forces (*38*). Results for the bacterial solids (*S. alga* and *S. putrefaciens*) show relatively higher solid-phase Sr^{2+} concentrations compared to the *S. alga*−HFO composite or pure HFO at any given $[Sr_D]/[H^{+}]$.

The apparent surface complex formation constants and maximum binding capacities, estimated from double reciprocal plots of the experimental data, for the sorption of Sr^{2+} by the two species of *Shewanella* (log $K^{S}_{Sr} = -0.51$ and -0.66, $BSr_{max} = 0.079$ and 0.075 mmol·g^{-1} for *S. alga* and *S. putrefaciens*, respectively) are significantly greater than the HFO binding constant and maximum sorptive capacity (log $K^{S}_{Sr} = -2.13$ and $BSr_{max} = 0.001$ mmol·g^{-1}, Table 1). The two orders of magnitude difference between the HFO and bacteria surface complex formation constants demonstrated that the Sr^{2+} sorption affinity of both bacteria greatly exceeds that of HFO. In addition, the maximum binding capacities of the bacteria were also approximately two orders of magnitude greater than the HFO, emphasizing the potential geochemical importance of bacteria in controlling contaminant fate in aqueous environments. These results further suggest that the sorptive capacities of different bacterial species, while variable, fall within similar orders of magnitude. The same behavior has been noted for Cd and Pb sorption to *Bacillus subtilis* and *Bacillus licheniformis* by Daughney et al. (*12*) and Fein et al. (*13*).

The apparent log K^{S}_{Sr} value of -2.13 calculated for Sr^{2+} sorption to HFO is greater than the reported value of Dzombak and Morel (*6*) for the mean intrinsic strontium surface complex formation constant (log $K_2 = -6.58$) corresponding to eq 1. Inherent differences in calculating apparent and intrinsic surface complex formation constants as well as differences in the age of the HFO, as fresh HFO precipitates (such as ours) are considered to be more chemically reactive

TABLE 1. Apparent Surface Complex Formation Constants (K^{S}_{Sr}) and Maximum Binding Capacities (BSr_{max}) for *S. alga*, *S. putrefaciens*, HFO, and *S. alga*−HFO Composite

substrate	log K^{S}_{Sr} [a]	BSr_{max} [b] (mmol·g^{-1})	r^2 [c]
S. alga (BrY)	−0.51	0.079	0.87
S. putrefaciens (CN-32)	−0.66	0.075	0.90
BrY + HFO	−0.68	0.034	0.84
HFO	−2.13	0.001	0.94

[a] Log K^{S}_{Sr}, apparent surface complex formation constant for each sorbent and Sr^{2+}. [b] BSr_{max}, the maximum mmol of Sr^{2+} that is sorbed to each sorbent per gram of solid. Values in footnotes *a* and *b* were calculated using line regression estimated from double reciprocal plots of the experimental sorption data shown in Figure 4. [c] r^2, values are correlation coefficients for the regression analyses (STATISTICA v. 5.0).

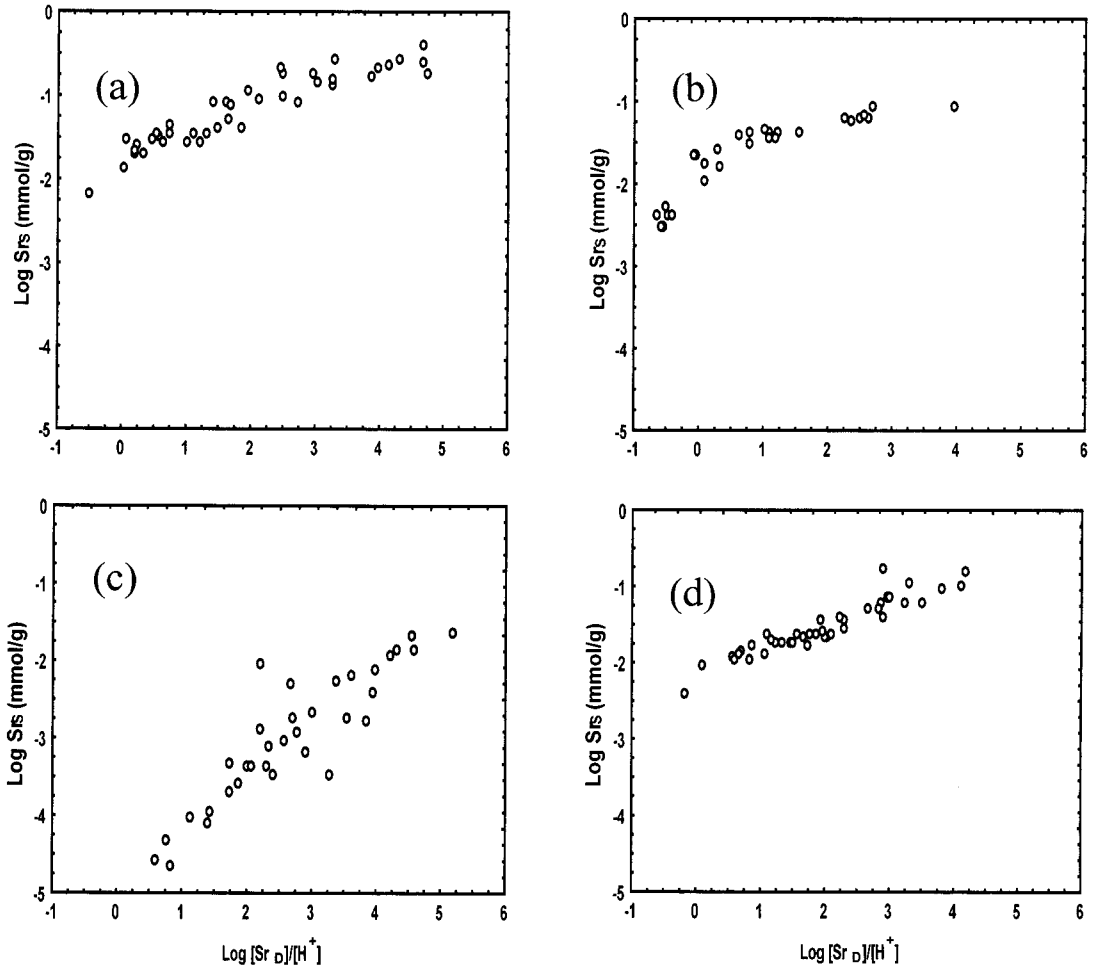

FIGURE 4. Log Sr_S (mmol/g) as a function of log $[Sr_D]/[H^+]$ for the four substrate systems: (a) *S. alga*, (b) *S. putrefaciens* (c) HFO, and (d) *S. alga*−HFO composite. The data points are averages from a series of experiments where the $[Sr_T]$ and pH were both varied.

than aged HFOs (*6*), may explain the differences between the two sorption constants.

In natural systems, heterogeneous organic−oxide complexes are usually found, resulting in solids that have the chemical characteristics of both the inorganic and organic phases (*10, 29*). The apparent surface complex formation constant for the *S. alga*−HFO composite in this study (log $K^S_{Sr} = -0.68$) is about the same as pure *S. alga* cells but higher than the pure HFO solid. As shown in Figure 4 and Table 1, the data set for the *S. alga*−HFO composite more closely resembles that of the pure bacterial substrate than the HFO. The maximum binding capacity for sorption of Sr^{2+} to the composite bacterial-HFO surface falls between the capacities observed for the bacteria and HFO separately (Table 1). The bacteria−HFO composite maximum binding capacity for Sr^{2+} was 0.034 mmol·g^{-1} which is 21% less than was calculated to be sorbed by the composite substrate (0.043 mmol·g^{-1}) based on the sorptive characteristics of each solid (bacteria and HFO) and their mass fraction in the composite solid. Assuming independent sorption behavior for *S. alga* and HFO, the calculated concentration of Sr^{2+} sorbed to the composite surface was calculated for any given $[Sr_D]/[H^+]$ by the equation (*38*)

$$Sr_S(\text{total}) = f_{HFO}(Sr_{S-HFO}) + f_{S.alga}(Sr_{S-S.alga}) \qquad (4)$$

where Sr_S(total) is the quantity of Sr^{2+} calculated to be sorbed to the composite solid, f_{HFO} and $f_{S.alga}$ are the weight fractions of HFO (0.30) and *S. alga* (0.70) comprising the composite solid, and Sr_{S-HFO} and $Sr_{S-S.alga}$ are the observed concentrations of Sr^{2+} sorbed to the individual sorbents (HFO and *S. alga*, respectively).

The calculated Sr_S values for the *S. alga*−HFO composite versus the observed Sr_S values for the *S. alga*−HFO composite show a strong linear trend but fall above and parallel to the 1:1 reference line indicating an overestimation of Sr_S compared to the concentration of Sr^{2+} actually sorbed to the *S. alga*−HFO composite (Figure 5). This relationship implies that the relative decrease in the sorptive capacity of the *S. alga*−HFO composite results from a masking of the bacterial Sr^{2+} binding sites by HFO. The decreased availability of the bacterial functional groups leads to a decreased overall sorptive capacity.

It has been demonstrated in natural environments that many bacteria are naturally coated with amorphous iron oxides (*32*) and that the proportion of HFO comprising the bacteriogenic iron oxide complex ultimately controls the composite substrate's ability to sorb metal ions (*29*). Although Figure 5 establishes that the *S. alga*−HFO complex sorbs less Sr^{2+} than expected, the influence that the proportion of HFO coating *S. alga* has on the composite surface Sr^{2+} scavenging abilities remains to be investigated.

The quantification of solid phase strontium partitioning at four sorbent surfaces was successfully described using the SCT approach and allowed for the first comparison among two bacterial species, an Fe oxide (HFO) and a composite bacterial-Fe oxide as potential sorbents. The scavenging of Sr^{2+} by all four surfaces was pH dependent showing rapid increases in Sr_S as pH increased. The results additionally showed that significant Sr^{2+} sorption occurred at the bacterial

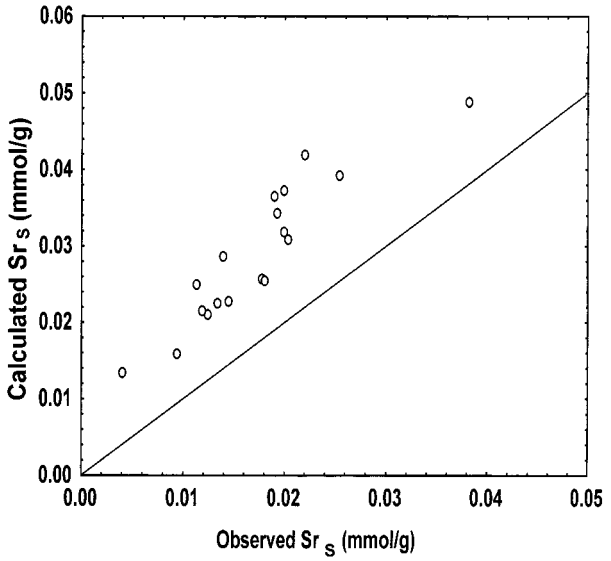

FIGURE 5. Observed [Sr_S (mmol·g^{-1})] plotted as a function of calculated [Sr_S (mmol·g^{-1})] for the bacteria−HFO complex showing a linear trend parallel to and above the solid 1:1 reference line, indicating an overestimation of Sr_S compared to the concentration of Sr^{2+} actually sorbed to the *S. alga*−HFO composite.

surfaces approximately 2 pH units lower than at the HFO surfaces. At the same time, the two *Shewanella* sp. exhibited remarkably similar affinities for Sr^{2+}, and both species were able to sorb significantly greater quantities of Sr^{2+} than the HFO (0.079 and 0.075 mmol·g^{-1} for *S. alga* and *S. putrefaciens*, respectively, compared to 0.001 mmol·g^{-1} for HFO). These observations provide quantitative evidence that bacteria can sorb Sr^{2+} at relatively low pH values and in greater quantities, compared to HFO surfaces, emphasizing their importance for contaminant modeling, and for possible remedial applications. The bacteria−HFO complex was found to be intermediate between the pure bacteria and HFO but showed a lower sorptive capacity than was calculated. This result is explained by a masking of bacterial sorption sites by the surface associated HFO, which has a lower relative sorptive capacity than the bacterial surface. Other results suggest that the amount of HFO precipitated in association with bacteria will ultimately determine the metal ion scavenging ability of the bacteria−HFO complex (*29*). However, the fundamental concept is that microbial mediated reactions involving dissolved inorganic contaminants must be considered if accurate contaminant fate models are to be developed.

Acknowledgments

This work was supported in full by Grant no. DE-FG07-96ER62317 Environmental Management Science Program, Office of Science and Technology, Office of Environmental Management, United States Department of Energy (DOE). We would like to thank Andrew Wolf for his assistance with the AAS and ICP-AES analyses and Nagina Parmar for microbial culture preparation. We would also like to thank N. Coombs for technical assistance with SEM and EDS analyses.

Literature Cited

(1) Davis, J. A.; Coston, J. A.; Kent, D. B.; Fuller, C. C. *Environ. Sci. Technol.* **1998**, *32*, 2820.
(2) Venema, P.; Hiemstra, T.; van Riemsdijk, W. H. *J. Colloid Interface Sci.* **1996**, *181*, 45.
(3) Robertson, A. P.; Leckie, J. O. *J. Colloid Interface Sci.* **1997**, *188*, 444.
(4) Wang, F.; Chen, J.; Forsling, W. *Environ. Sci. Technol.* **1997**, *31*, 448.
(5) Wen, X.; Du, Q.; Tang, H. *Environ. Sci. Technol.* **1998**, *32*, 870.
(6) Dzombak, D. A.; Morel, F. M. M. *Surface Complexation Modeling: Hydrous Ferric Oxide*; Wiley-Interscience: New York, 1990.
(7) Davis, J. A.; Kent, D. B. In *Mineral-Water Interface Geochemistry;* Hochella, M. F., Jr.; White, A. F., Eds.; Rev. Mineral. 1990; Vol. 23, Chapter 5.
(8) Saunders, J. A.; Toran, L. E. *Appl. Geochem.* **1995**, *10*, 673.
(9) Comans, R. N. J.; Middelburg, J. J. *Geochim. Cosmochim. Acta* **1987**, *51*, 2587.
(10) Tessier, A.; Fortin, D.; Belzile, N.; DeVitre, R. R.; Leppard, G. G. *Geochim. Cosmochim. Acta* **1996**, *60*, 387.
(11) Catis, J. G.; Langmuir, D. *Appl. Geochem.* **1986**, *1*, 255.
(12) Daughney, C. J.; Fein, J. B.; Yee, N. *Chem. Geol.* **1998**, *144*, 161.
(13) Fein, J. B.; Daughney, C. J.; Yee, N.; Davis, T. A. *Geochim. Cosmochim. Acta* **1997**, *61*, 3319.
(14) Warren, L. A.; Ferris, F. G. *Environ. Sci. Technol.* **1998**, *32*, 2331.
(15) Bradley, D. J.; Frank, C. W.; Mikevin, Y. *Phys. Today* **1996**, *49*, 40.
(16) Stumm, W.; Sigg, L.; Sulzberger, B. In *Chemical and Biological Regulation of Aquatic Systems;* Buffle, J., DeVitre, R., Eds.; Lewis: Boca Raton, 1994; Chapter 2.
(17) Hu, M. Z.-C.; Norman, J. M.; Faison, B. D.; Reeves, M. E. *Biotech. Bioeng.* **1996**, *51*, 237.
(18) Mullen, M. D.; Wolf, D. C.; Ferris, F. G.; Beveridge, T. J.; Flemming, C. A.; Bailey, G. W. *Appl. Environ. Microbiol.* **1989**, *55*, 3143.
(19) Urrutia, M. M.; Roden, E. E.; Fredrickson, J. K.; Zachara, J. M. *Geomicrobiol.* **1998**, *15*, 269.
(20) Ledin, M.; Pedersen, K.; Allard, B. *Water Air Soil Pollut.* **1997**, *93*, 367.
(21) Doyle, R. J.; Matthews, T. H.; Streips, U. N. *J. Bacteriol.* **1980**, *143*, 471.
(22) Avery, S. V.; Tobin, J. M. *Appl. Environ. Microbiol.* **1992**, *58*, 3883.
(23) Brady, J. M.; Tobin, J. M. *Enzyme Microbiol. Technol.* **1994**, *16*, 671.
(24) Urrutia, M. M. In *Biosorbens for Metal Ions*; Wase, J., Forster, C., Eds.; Taylor and Francis: London, 1997; Chapter 3.
(25) Beveridge, T. J. In *Metal Ions and Bacteria*; Beveridge, T. J., Doyle, R. J., Eds.; John Wiley and Sons: New York, 1989; Chapter 1.
(26) Ferris, F. G. In *Metal Ions and Bacteria*; Beveridge, T. J., Doyle, R. J., Eds.; John Wiley and Sons: New York, 1989; Chapter 10.
(27) Ferris, F. G. In *Biological-Mineralogical Interactions*; McIntosh, J. M., Groat, L. A., Eds.; Mineralogical Association of Canada: 1997; Vol. 25, Chapter 9.
(28) Beveridge, T. J.; Hughes, M. N.; Lee, H.; Leueng, K. T.; Poole, P. K.; Sauvaidis, I.; Silver, S.; Trevors, J. T. *Adv. Microb. Phys.* **1997**, *38*, 177.
(29) Ferris, F. G.; Konhauser, K. O.; Lyven, B.; Pedersen, K. *Geomicrobiol. J.* **1999**, *16*, 181.
(30) Ferris, F. G.; Beveridge, T. J.; Fyfe, W. S. *Nature* **1986**, *320*, 609.
(31) Fortin, D.; Ferris, F. G. *Geomicrobiol. J.* **1998**, *15*, 309.
(32) Konhauser, K. O. *Earth-Science Rev.* **1998**, *43*, 91.
(33) Caccavo, F. Jr.; Schamberger, P. C.; Keiding, K.; Nielsen, P. H. *Appl. Environ. Microbiol.* **1997**, *63*, 3837.
(34) Honeyman, B. D.; Santschi, P. H. *Environ. Sci. Technol.* **1988**, *22*, 862.
(35) Caccavo, F. Jr.; Blakemore, R. P.; Lovley, D. R. *Appl. Environ. Microbiol.* **1992**, *58*, 3211.
(36) Caccavo, F., Jr.; Ramsing, N. B.; Costerton, J. W. *Appl. Environ. Microbiol.* **1996**, *62*, 4678.
(37) Nealson, K. H.; Saffarini, D. *Annu. Rev. Microbiol.* **1994**, *48*, 311.
(38) Stumm, W.; Morgan, J. J. *Aquatic Chemistry*, 3rd ed.; Wiley-Interscience: New York, 1996.

Received for review May 18, 1999. Revised manuscript received September 10, 1999. Accepted September 13, 1999.

ES9905694